CCP4 NEWSLETTER ON PROTEIN CRYSTALLOGRAPHY

An informal Newsletter associated with the BBSRC Collaborative Computational Project No. 4 on Protein Crystallography.

Number 39 **March 2001**

Contents

1. **News from CCP4**
   Peter Briggs, Martyn Winn, Sue Bailey, Alun Ashton, David Brown, Charles Ballard
2. **SC: measuring shape complementarity at protein-protein interfaces**
   Mike Lawrence
3. **ANISOANL - analysing anisotropic displacement parameters**
   Martyn Winn
4. **LAPACK in CCP4 4.1**
   Peter Briggs
5. **A System for storing Annotated Diffraction Data**
   John Badger
6. **CCP4 Molecular Graphics**
   Liz Potterton
7. **ARP/wARP goes CCP4i**
   Anastassis Perrakis, Liz Potterton and Victor Lamzin
8. **Vector-Search Methods in Molecular Replacement**
   Carmen Álvarez-Rúa, Javier Borge and Santiago García-Granda
9. **MAPSLICER: an interactive viewer for contoured map sections**
   Peter Briggs
10. **Protein Crystallography Specialist Users Group Meeting**
    Pierre Rizkallah
11. **Maximum-Likelihood Refinement of Atomic Models using Least-Squares Criterion**
    P. Afonine, V.Y. Lunin and A. Urzhumtsev
12. **CCP4i Chart Interface**
    Paul Emsley
13. **Efficient calculation of the exact matrix of the second derivatives**
    Alexandre G. Urzhumtsev and Vladimir Y. Lunin
14. **Reports from the Daresbury Protein Crystallography Data Collection Workshop**
    Liz Duke and Jasveen Chugh
15. **Improvement of noisy maps by bulk solvent correction**
    A. Fokine and A. Urzhumtsev
16. **Multiple rotation function**
    L. Urzhumtseva & A. Urzhumtsev
17. **An Open Source Multi-purpose Programming Environment for Macromolecular Crystallography**
    Thomas Hamelryck and Morten Kjeldgaard
18. **Recent improvements to Mosflm - version 6.11**
    Harry Powell

19. **Recent CCP4BB Discussions**
Maria Turkenburg
20. **CCP4/Max-INF Workshop on Refinement and Validation of Macromolecular Structure**
Eleanor Dodson

Editor: Peter Briggs Daresbury Laboratory, Daresbury, Warrington, WA4 4AD, UK

NOTE: The CCP4 Newsletter is not a formal publication and permission to refer to or quote from the articles reproduced here must be referred to the authors.

Contributions are invited for the next issue of the newsletter, and should be sent to Charles Ballard by e-mail at c.c.ballard@ccp4.ac.uk by 31st August 2001. HTML is preferred but other formats are also acceptable.

CCP4 Main Page

Newsletter contents...

Improvement of noisy maps by bulk solvent correction

By A. Fokine & A. Urzhumtsev

Laboratory of Crystallography and Modelling of Mineral and Biological Materials, UPRESA 7036 CNRS, University Henri Poincarй, Nancy I, 54506 Vandoeuvre-les-Nancy, France

e-mail : sacha@lcm3b.u-nancy.fr

Introduction

The main goal of the structural crystallography is to build a model of the crystal under study. For macromolecules, to do so an electron density map calculated at a finite resolution, as high as possible, is necessary. A distribution of the electron density in a crystal can be represented by a Fourier series with the coefficients $\mathbf{F}_{\mathbf{obs}}$ the main contribution to which comes from ordered atoms, $\mathbf{F}_{\mathbf{atom}}$, and from bulk solvent, $\mathbf{F}_{\mathbf{solv}}$:

$$\mathbf{F}_{\mathbf{obs}} = \mathbf{F}_{\mathbf{atom}} + \mathbf{F}_{\mathbf{solv}} . \qquad (1)$$

The complex values $\mathbf{F}_{\mathbf{obs}}$ are not available from a single X-ray diffraction experiment and usually they are approximated by

$$\mathbf{F}_{\mathbf{obs}} \sim |\mathbf{F}_{\mathbf{obs}}|\exp(i\varphi_{est}) \qquad (2)$$

where φ_{est} are some estimations for structure-factor phases.

However, since the main goal of the map interpretation is to build an atomic model, it seems that the map calculated with the coefficients $\mathbf{F}_{\mathbf{atom}}$ should be more suitable for this purpose (Urzhumtsev, 2000) than the traditional map calculated with the coefficients (2). If we assume that the bulk solvent contribution to the diffraction pattern can be estimated before an atomic model is known, these structure factors can be approximated as

$$\mathbf{F}_{\mathbf{atom}} \sim (|\mathbf{F}_{\mathbf{obs}}|\exp(i\varphi_{est}) - \mathbf{F}_{\mathbf{solv}}). \qquad (3)$$

It should be noted that the substitution $(|\mathbf{F}_{\mathbf{obs}}|\exp(i\varphi_{est}) - \mathbf{F}_{\mathbf{solv}})$ for $|\mathbf{F}_{\mathbf{obs}}|\exp(i\varphi_{est})$ changes not only the phases of the Fourier coefficients but also their moduli, differently from standard phase improvement methods (taking apart weighting of moduli by figure of merit of corresponding phase).

The numerical tests discussed below show that such map correction by subtraction of the bulk solvent contribution can significantly improve the quality of density maps. For such study, we

simulated the problem arising in the single isomorphous replacement (SIR) method and analysed the quality of SIR maps, calculated before and after bulk solvent contribution, as a function of resolution and error in the position of the heavy atom.

Tests description

Atomic model

The crystal structure of Fab fragment of monoclonal antibody LNKB-2 solved at 2.2 E resolution (Fokin *et al*., 2000) was chosen as a test model. Crystals of Fab-LNKB-2 belong to the space group $P2_12_12_1$ (a = 72.24 E, b = 72.01 E, c = 86.99 E) and contain one molecule per asymmetric unit. Solvent region occupies 42% of the unit cell volume. Fab fragment molecule consists of two polypeptide chains (with 219 and 220 amino acid residues, respectively). 213 water molecules are included in the atomic model.

Solvent structure

In order to simulate the contribution of the bulk solvent we used the approach by Jiang & Brьnger (1994). A binary solvent mask (1 in solvent region 0 in protein region) was calculated by program CNS (Brunger *et al*., 1998) with the parameters SOLRAD and SHRINK equal to 1.0 E. The corresponding structure factors $\mathbf{F_{mask}}$ were exponentially scaled

$$\mathbf{F_{solv}} = k_{sol} \exp(-B_{sol}\sin^2(\theta)/\lambda^2)\, \mathbf{F_{mask}} \qquad (4)$$

with scaling parameters k_{sol} and B_{sol} chosen as 0.40 e^-/ E^3 and 70 E^2 , respectively.

The structure factors $\mathbf{F_{solv}}$ of the bulk solvent were then added to structure factors $\mathbf{F_{atom}}$ calculated from the atomic model giving the total structure factors of the crystal

$$\mathbf{F_{tot}} = \mathbf{F_{atom}} + \mathbf{F_{solv}}. \qquad (5)$$

Each set of structure factors included 23673 reflections and corresponded to the full data set up to 2.2 E resolution.

Numerical SIR simulation

A SIR-like situation was simulated as it was described previously in (Urzhumtsev, 1991). An artificial gaussian heavy atom was placed in the cavity between two variable and two constant domains of Fab molecule. For this artificial heavy-atom derivative structure factors $\mathbf{F_{der}}$ were calculated as

$$\mathbf{F_{der}} = \mathbf{F_{tot}} + \mathbf{F_H} \qquad (6)$$

where $\mathbf{F_H}$ are structure factors for the heavy atom. The number of electrons in the heavy atom was chosen such that its contribution to the structure factors was

$$R_H = \Sigma|\mathbf{F_H}| / \Sigma|\mathbf{F_{tot}}| = 0.1\ . \qquad (7)$$

In the tests, the moduli of structure factors $\mathbf{F_{tot}}$ and $\mathbf{F_{der}}$ were supposed to be known and simulated the experimental magnitudes for the native crystal and its derivative. The position of heavy atom was supposed to be determined either absolutely accurately or with the coordinate error of 1.0 or 2.0 E, depending on the test. The $|\mathbf{F_{tot}}|$ and $|\mathbf{F_{der}}|$ values and heavy atom parameters were used to calculate phases φ_{sir} and their figures of merit m_{sir} with the standard SIR technique (Blow & Rossman, 1961).

Electron density maps

SIR-phased Fourier syntheses

$$\rho_{sir}(\mathbf{r}) = V^{-1}\{\Sigma_{\mathbf{h}}\, m_{sir}|\mathbf{F_{tot}}(\mathbf{h})|\exp(i\varphi_{sir}(\mathbf{h}))\exp(-2\pi i\mathbf{hr})\} \quad (8)$$

and the syntheses with subtracted bulk solvent contribution

$$\rho_{corr}(r) = V^{-1}\{\Sigma_{\mathbf{h}}\,[\, m_{sir}|\mathbf{F_{tot}(h)}|\exp(i\varphi_{sir}(\mathbf{h})) - \mathbf{F_{solv}}\,]\exp(-2\pi i\mathbf{hr})\} \quad (9)$$

were calculated using reflections with the resolution $d > d_{min}$, where d_{min} was equal to 2.2, 3.0, and 6.0 E depending on the test (here V is the unit cell volume). For comparison we calculated also the maps with the coefficients $\mathbf{F_{atom}}$

$$\rho_{atom}(r) = V^{-1}[\Sigma_{\mathbf{h}}\,\mathbf{F_{atom}}(\mathbf{h})\exp(-2\pi i\mathbf{hr})]. \quad (10)$$

All syntheses were normalised with respect to their mean value and standard deviation σ.

Numerical comparison of electron density maps

When Fourier syntheses $\rho(r)$ are analysed, the objects of interest are the shape and localisation of equipotential surfaces rather than the absolute values of the density. The lower is the cut-off level ρ^*, the larger is the region bounded by the surface $\rho(r) = \rho^*$, the more atoms of the model are inside (trapped by) this region. On another hand, when comparing two synthesis taken at an equivalent level, the better one traps more atoms than the worse one. Therefore, the percentage of the missed atoms $D(\rho)$ as a function of cut-off level can be used to estimate the quality of the syntheses as it is realised in the program MTRAP (Lunina & Lunin, personal communication). While originally in MTRAP the cut-off level is estimated through the relative volume of the selected region, for our tests we used more traditional measure in sigmas.

Results and discussion

Figure 1 illustrates the quality of the maps calculated at 6.0, 3.0, and 2.2 E resolution with exactly assigned position of the heavy atom. The syntheses with subtracted bulk solvent contribution are significantly better than standard SIR syntheses (compare solid and dotted lines, Fig. 1). The effect of the map improvement due to subtraction of the bulk solvent contribution depends on the resolution and on the level of the equipotential surfaces. For the map calculated at 6.0 E resolution (Fig.1a) the improvement is significant for levels in the interval 0-1 σ, and for maps calculated at 3.0 E and 2.2 E resolution (Figs. 1b, 1c) the improvement is significant for levels in the interval 0-1.5 σ. At higher levels we will see only a small number of strong peaks

corresponding to clearly observed atoms. The improvement is maximal for the SIR synthesis calculated at 6.0 E resolution (compare solid and dotted lines, Fig. 1a). For example, at 0.5 σ the percentage of missed atoms for SIR synthesis is 50 but for the synthesis with subtracted bulk solvent contribution it is less than 20. This is not surprising because the bulk solvent contribution is very significant at low resolution.

The maps calculated with 1.0 E error in the heavy atom position (Fig. 2) are of lower quality than the corresponding SIR maps calculated with the exact position of the heavy atom (compare dotted lines at Figs. 1 and 2). Higher-resolution SIR syntheses are quite sensitive to this error; for example, at 1.0 σ the share of missed atoms in the SIR synthesis calculated at 2.2 E resolution increases from 20% to 50% (dotted lines, Figs. 1c and 2c). On the other hand the quality of the SIR map calculated at 6.0 E resolution does not change significantly (dotted lines, Figs. 1a and 2a). As previously for the exact heavy atom position, the subtraction of the bulk solvent contribution significantly improves the maps quality (compare dotted and solid lines Fig. 2a, 2b, 2c).

Because low resolution phases are less sensitive to the error in the heavy-atom position, when this error reaches 2.0 E (Fig. 3) the quality of the SIR map calculated at 6.0 E resolution becomes even better then the quality of SIR maps calculated at 3.0 E and 2.2 E. The most significant improvement after subtraction of the bulk solvent contribution corresponds also to the 6.0 E resolution synthesis.

Fig. 4a shows the SIR electron density map and the atomic model superimposed. The map contains many noisy peaks in the solvent region. After subtraction of the bulk solvent contribution practically all these peaks in the solvent region disappear (Fig. 4b) which is not surprising. More important is that the map becomes better in the regions of the macromolecule as illustrated in more details in Figs. 5 and 6. A region of the light chain of Fab fragment is shown in the SIR map (Fig. 5a) and in the map with the subtracted bulk solvent contribution (Fig. 5b). After the correction many noisy peaks disappear from the map and the correct electron density appears for residues Gly1 and Val2 where it was absent previously. The same maps show also a significant improvement of the image quality in the region of the heavy chain, for example for the residues Gln77 and Phe79 (Fig. 6).

It can be also noted that the subtraction of the solvent contribution does not change the sharpness of the map; in all cases the maximum value of the map expressed in sigmas is practically conserved. Therefore, the improvement of the model trapping is indeed due to an improvement of molecular contours in the map.

Conclusions

Our tests show that if the bulk solvent contribution to the diffraction pattern is known at early stages of phasing, the quality of the electron density maps can be significantly improved by subtraction of this contribution. The most significant improvement is observed for syntheses calculated at low resolution with large errors in heavy atom position, because the bulk solvent contribution is more significant at low resolution and low resolution synthesis are less sensitive to errors in the heavy atom position.

Currently, the bulk solvent contribution is estimated only when a (preliminary) atomic model is available and used mostly to refine this model. The use of the bulk solvent contribution for map correction needs to develop more sophisticated methods for its estimation without use of atomic models (work in progress).

The authors thank Prof. C. Lecomte for his interest to the project and L. Torlay for technical help. The work was supported through CPER, Pole ``Intellegence Logicielle".

References

Blow, D.M. & Rossmann M.G. (1961) *Acta Cryst.,* **14**, 1195-1202.

Brьnger, A.T., Adams, P.D., Clore, G.M., DeLabo, W.L., Gros, P., Grosse-Kunstleve, R.W., Jiang, J.-S., Kuszewski, J., Nilges, M., Pannu, N.S., Read, R.J., Rice, L.M., Simonson, T. & Warren, G.L. (1998) *Acta Cryst.,* D**54**, 905-921.

Fokine, A.V., Afonine, P.V., Mikhailova, I.Yu., Tsygannik, I.N., Mareeva, T.Yu., Nesmeyanov, V.A., Pangborn, W., Li, N., Duax, W., Siszak, E., Pletnev, V.Z. (2000). *Rus. J. Bioorgan. Chem.*, **26**, 512-519.

Guex, N. & Peitsch, M.C. (1997) *Electrophoresis*, **18**, 2714-2723.

Jiang, J.S. & Brьnger A.T.(1994) *J. Mol. Biol.,* **243**, 100-115.
Jones, T.A. (1978) *J. Appl. Crystallogr.,* **11**, 268-272.
Urzhumtsev, A.G. (1991) *Acta Cryst.*, **A47**, 794-801

Urzhumtsev, A.G. (2000) *CCP4 Newsletter on Protein Crystallography,* **38**, 38-49.

Figures

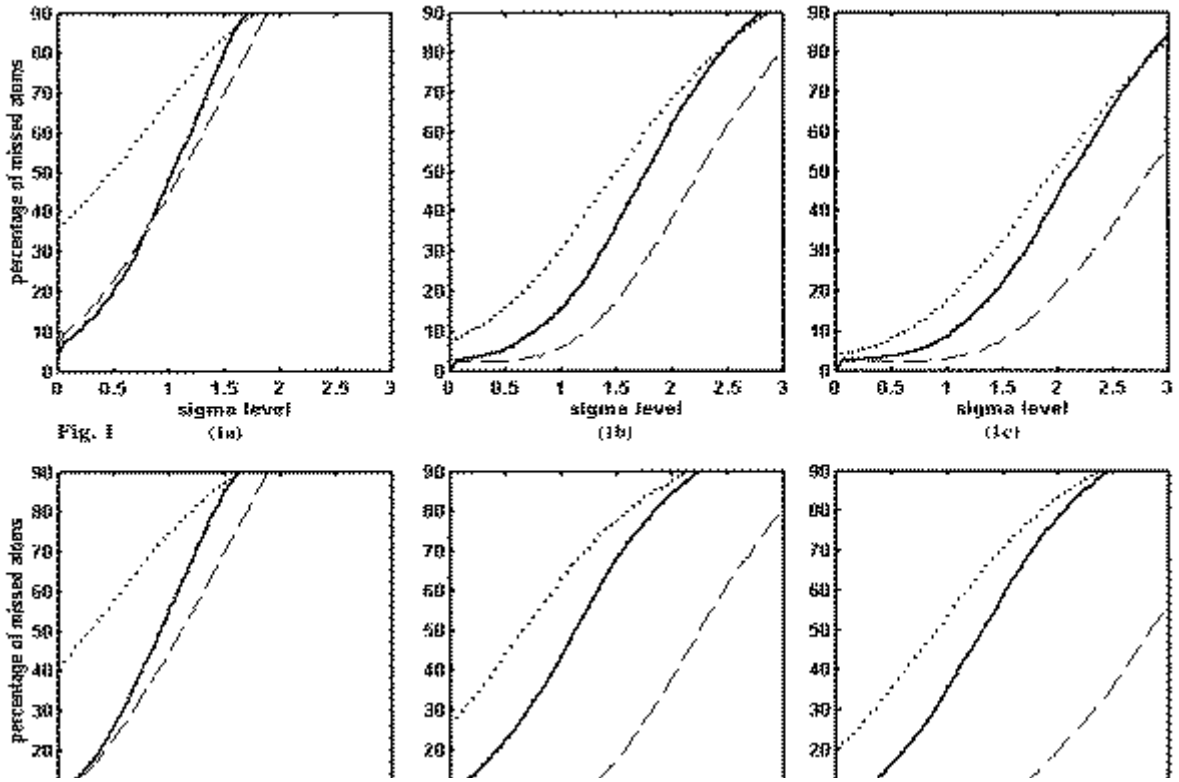

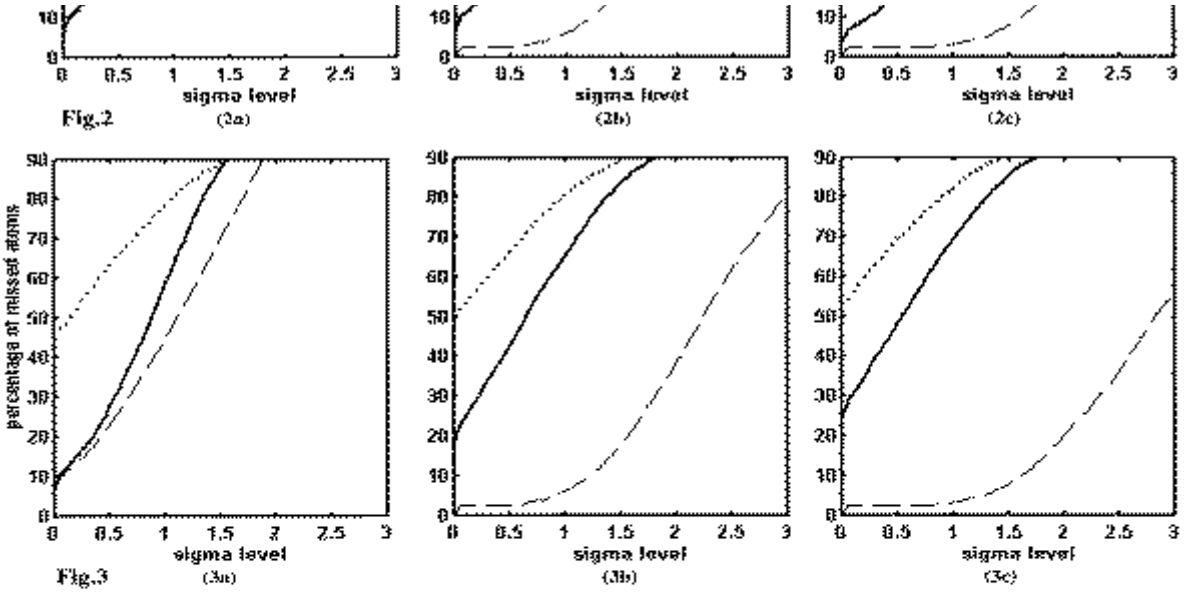

Fig. 1, 2, 3. Percentage of missed atoms depending on sigma level of equipotential surface.
Dotted lines: Maps calculated with the coefficients $m_{sir}|\mathbf{F_{tot}}|\exp(i\varphi_{sir})$.
Solid lines: Maps calculated with the coefficients $m_{sir}|\mathbf{F_{tot}}|\exp(i\varphi_{sir})-\mathbf{F_{solv}}$.
Dashed lines: Maps calculated with the coefficients $\mathbf{F_{atom}}$.

(1a), (1b), (1c) - position of heavy atom is exactly determined.
(2a), (2b), (2c) - position of heavy atom is determined with the error of 1.0 Å.
(3a), (3b), (3c) - position of heavy atom is determined with the error of 2.0 Å.

(1a), (2a), (3a) - maps calculated at 6.0 Å resolution.
(1b), (2b), (3b) - maps calculated at 3.0 Å resolution.
(1c), (2c), (3c) - maps calculated at 2.2 Å resolution.

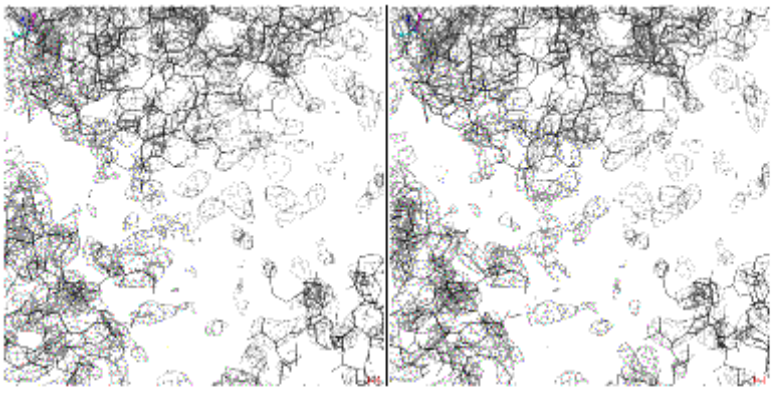

(4a)

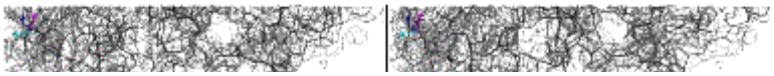

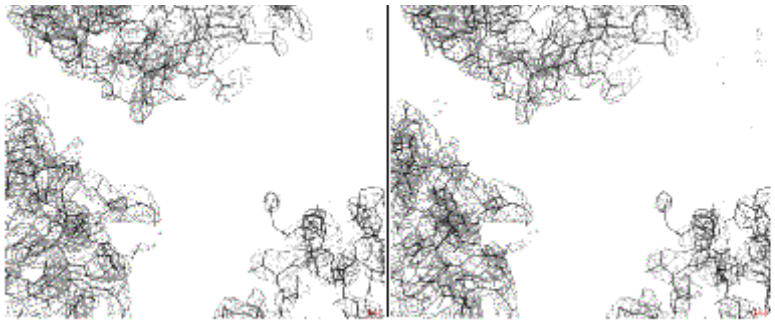

(4b)

Fig. 4 Stereo-view of the atomic model (Fab LNKB-2) superimposed with electron density maps calculated at 3.0Å resolution with exact heavy atom position. Equipotential surfaces at the level 1.5 sigma are shown. The figure was done using the program CHAIN (Jones, 1978).

(4a) - map calculated with the coefficients $m_{sir}|\mathbf{F_{tot}}|\exp(i\varphi_{sir})$.

(4b) - map calculated with the coefficients $m_{sir}|\mathbf{F_{tot}(h)}|\exp(i\varphi_{sir})-\mathbf{F_{solv}}$.

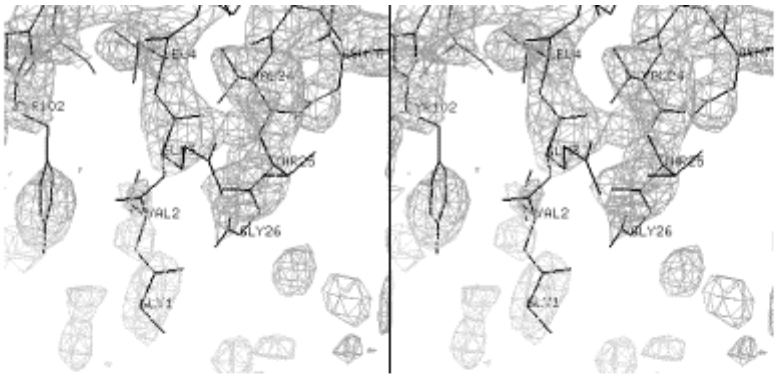

(5a)

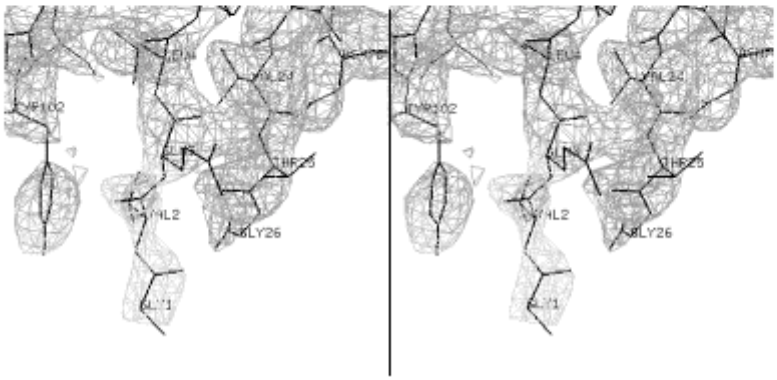

(5b)

Fig. 5 Stereo-view of a fragment of the light chain of Fab LNKB-2 superimposed with electron density maps calculated at 3.0 Å resolution with exact heavy atom position. Equipotential surfaces at the level 1.5 sigma are shown. The figure was done using the program Swiss-Pdb-Viewer (Guex & Peitsch, 1997).
(5a) - map calculated with the coefficients $m_{sir}|\mathbf{F_{tot}}|\exp(i\varphi_{sir})$.

(5b) - map calculated with the coefficients $m_{sir}|\mathbf{F_{tot}(h)}|\exp(i\varphi_{sir})-\mathbf{F_{solv}}$.

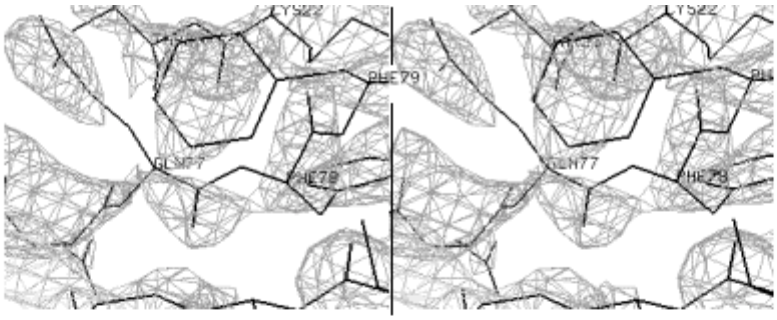

(6a)

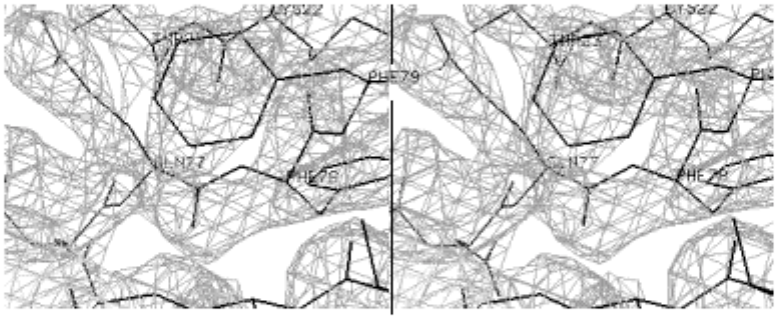

(6b)

Fig. 6 Stereo-view of a fragment of the heavy chain of Fab LNKB-2 superimposed with electron density maps calculated at 3.0 Å resolution with exact heavy atom position. Equipotential surfaces at the level 1.5 sigma are shown. The figure was done using the program Swiss-Pdb-Viewer (Guex & Peitsch,1997).
(6a) - map calculated with the coefficients $m_{sir}|\mathbf{F_{tot}}|\exp(i\varphi_{sir})$.

(6b) - map calculated with the coefficients $m_{sir}|\mathbf{F_{tot}(h)}|\exp(i\varphi_{sir})-\mathbf{F_{solv}}$.

Newsletter contents...